Title

Effects of abstinence and chronic cigarette smoking on white matter microstructure in alcohol dependence: Diffusion tensor imaging at 4T

Authors

Zou, Yukai
Murray, Donna E
Durazzo, Timothy C
et al.

Publication Date

2017-06-01

DOI

10.1016/j.drugalcdep.2017.01.032

Peer reviewed

Drug and Alcohol Dependence 175 (2017) 42–50

Contents lists available at ScienceDirect

Drug and Alcohol Dependence

journal homepage: www.elsevier.com/locate/drugalcdep

Full length article

Effects of abstinence and chronic cigarette smoking on white matter microstructure in alcohol dependence: Diffusion tensor imaging at 4 T

Yukai Zou[a,b,*], Donna E. Murray[c,d], Timothy C. Durazzo[e,f], Thomas P. Schmidt[d], Troy A. Murray[d], Dieter J. Meyerhoff[c,d]

[a] Weldon School of Biomedical Engineering, Purdue University, West Lafayette, IN 47906, United States
[b] College of Veterinary Medicine, Purdue University, West Lafayette, IN 47906, United States
[c] Department of Radiology and Biomedical Imaging, University of California San Francisco, San Francisco, CA 94143, United States
[d] Center for Imaging of Neurodegenerative Diseases (CIND), San Francisco VA Medical Center, San Francisco, CA 94121, United States
[e] Department of Psychiatry and Behavioral Sciences, Stanford University School of Medicine, Stanford, CA 94305, United States
[f] Mental Illness Research Mental Illness Research and Education Clinical Centers, Sierra-Pacific War Related Illness and Injury Study Center, VA Palo Alto Health Care System, Palo Alto, CA 94304, United States

ARTICLE INFO

Article history:
Received 11 July 2016
Received in revised form
21 December 2016
Accepted 22 January 2017
Available online 19 March 2017

Keywords:
Alcohol use disorder
Cigarette smoking
Behavior
Brain MRI
Diffusion tensor imaging
Tract-based spatial statistics (TBSS)

ABSTRACT

Background: We previously reported widespread microstructural deficits of brain white matter in alcohol-dependent individuals (ALC) compared to light drinkers in a small 1.5 T diffusion tensor imaging study employing tract-based spatial statistics. Using a larger dataset acquired at 4 T, the present study is an extension that investigated the effects of alcohol consumption, abstinence from alcohol, and comorbid cigarette smoking on white matter microstructure.
Methods: Tract-based spatial statistics were performed on 20 1-week-abstinent ALC, 52 1-month-abstinent ALC, and 30 controls. Regional measures of fractional anisotropy (FA) and mean diffusivity (MD) in the significant clusters were compared by Analysis of Covariance. The metrics were correlated with substance use history and behavioral measures.
Results: 1-week-abstinent ALC showed lower FA than controls in the corpus callosum, right cingulum, external capsule, and hippocampus. At 1 month of abstinence, only the FA in the body of the corpus callosum of ALC remained significantly different from controls. Some regional FA deficits correlated with more severe measures of drinking and smoking histories but only weakly with mood and impulsivity measures.
Conclusion: White matter microstructure is abnormal during early abstinence in alcohol dependent treatment seekers and recovers into the normal range within about four weeks. The compromised white matter was related to substance use severity, mood, and impulsivity. Our findings suggest that ALC may benefit from interventions that facilitate normalization of DTI metrics to maintain abstinence, via smoking cessation, cognitive-based therapy, and perhaps pharmacology to support remyelination.

1. Introduction

Alcohol dependence is associated with significant brain injury, negative health consequences (Sullivan, 2000; Oscar-Berman and Marinkovic, 2003; Zahr, 2014), and nearly 88,000 annual deaths in the United States (NIAAA, 2015). Around 80% of the alcohol-dependent individuals in North America also smoke cigarettes (Romberger and Grant, 2004; Durazzo and Meyerhoff, 2007). Cigarette smoking by itself has detrimental effects on neurobiology and cognition (Bolego et al., 2002; Hawkins et al., 2002; Garey et al., 2004; Durazzo et al., 2014a,b). In the United States, approximately 400,000 people die from cigarette smoking every year (Giovino, 2002), making it one of the largest preventable causes of death (Danaei et al., 2009).

Magnetic Resonance Imaging (MRI) can assess non-invasively the morphometry of brain tissue in alcohol use disorders (AUD) (Zahr, 2014). Macrostructural MRI studies of AUD described loss of gray matter (GM) and white matter (WM) volume (Pfefferbaum et al., 1992; Rohlfing et al., 2006; Bühler and Mann, 2011; Demirakca et al., 2011). A meta-analysis reported smaller GM volumes in alcohol-dependent individuals compared to controls in

* Corresponding author at: Weldon School of Biomedical Engineering, Purdue University, 206 S. Martin Jischke Drive, West Lafayette, IN 47907-2032, United States.
E-mail address: yukaizou2012@gmail.com (Y. Zou).

http://dx.doi.org/10.1016/j.drugalcdep.2017.01.032
0376-8716/

the prefrontal cortex, posterior cingulate cortex, and dorsal striatum (Xiao et al., 2015). Longitudinal MRI studies showed partially reversible brain tissue loss with abstinence from alcohol, and the underlying mechanisms likely involve remyelination and glial cell proliferation (Sullivan and Pfefferbaum, 2005; Crews and Nixon, 2009). Recently, we reported WM volume recovery in alcohol-dependent individuals over 7.5 months of abstinence, and frontal WM showed the greatest change during the change over the first month of abstinence (Durazzo et al., 2015).

Magnetic resonance-based diffusion tensor imaging (DTI) can assess damage to the microstructure of WM tissue, potentially reflecting fiber organization and myelin changes in the brain (Basser et al., 1994; Mori and Zhang, 2006). Fractional anisotropy (FA), a common DTI metric, is sensitive to neuronal characteristics such as the axonal size, density, and myelination, while mean diffusivity (MD) reflects the magnitude of water diffusion (Beaulieu, 2002; Mori and Zhang, 2006; Wozniak and Lim, 2006; Wheeler-Kingshott and Cercignani, 2009; Jbabdi et al., 2010; Jeurissen et al., 2013). WM fibers without pathology or injury typically show relatively high FA, as the intact myelin layers restrict the directions of water diffusion; lower FA (and the typically associated higher MD) indicates less directed water diffusion and may suggest fiber demyelination in pathological states (Pfefferbaum and Sullivan, 2005; Zahr, 2014). Widespread age-dependent microstructural abnormalities have been reported in AUD via DTI and interpreted to potentially reflect damage to myelin and axons (Pfefferbaum et al., 2006; Yeh et al., 2009; Zahr, 2014; Sorg et al., 2015).

Tract-Based Spatial Statistics (TBSS) is a DTI analysis method that creates a mean FA skeleton representing the major fiber bundles connecting different cortical brain regions. It minimizes the effects of geometric distortion from data acquisition, reduces partial volume effects, and therefore improves the power of detecting regional FA differences at group level (Smith et al., 2006; Bach et al., 2014). We applied TBSS for determining microstructural differences between treatment-seeking alcohol-dependent individuals and light drinkers: FA was lower in fibers within frontal WM, limbic pathways, and between cortico-striatal regions; in the small group of patients, associations between drinking severity and regional FA were insignificant (Yeh et al., 2009). Other TBSS studies in alcohol dependence reported FA deficits specifically within cingulum, corpus callosum, fornix (Durkee et al., 2013; Trivedi et al., 2013; Pfefferbaum et al., 2014; Smith et al., 2015; Sorg et al., 2015), and superior longitudinal fasciculus (Pfefferbaum et al., 2014; Segobin et al., 2015). Microstructural abnormalities were most pronounced in major tracts within frontal WM (Fortier et al., 2014; Pfefferbaum et al., 2014; Sorg et al., 2015) and related to higher lifetime alcohol consumption (Sorg et al., 2015).

Contrary to the rather consistent findings of lower FA in AUD, both higher and lower regional FA was shown in chronic cigarette smokers. FA was *lower* in smokers than non-smokers within prefrontal WM and fronto-striatal fibers (Zhang et al., 2011), corpus callosum, anterior internal capsule, and the projection fibers connecting frontal cortices (Lin et al., 2013; Savjani et al., 2014). Others reported *higher* FA in smokers than non-smokers within right prefrontal WM, cingulum, and corpus callosum (Paul et al., 2008; Hudkins et al., 2012), fronto-parietal tracts and superior longitudinal fasciculus (Liao et al., 2011), internal and external capsules, and superior corona radiata (Yu et al., 2015).

To date, few DTI studies have addressed the influence of comorbid tobacco use on brain microstructure in AUD. In a large study of heavy drinkers, cigarette smoking did not affect WM microstructure significantly (Monnig et al., 2015). In a small longitudinal study of alcohol-dependent individuals between one and four weeks of abstinence, we detected trends to FA increases within frontal and temporal WM in non-smokers but not in smokers (Gazdzinski et al., 2010). These analyses suggest that smoking adversely affects WM microstructure and hinders its recovery during abstinence from alcohol. Correspondingly, using MR spectroscopy, we detected lower concentrations of *N*-acetylaspartate (NAA), a marker of neuron health and viability (Miller, 1991; Schuff et al., 2001; Meyerhoff, 2014), within frontal WM of smoking versus non-smoking alcohol-dependent individuals (Wang et al., 2009; Durazzo et al., 2013); longitudinal recovery of NAA during alcohol abstinence was greater in the non-smoking than smoking individuals (for review see Meyerhoff, 2014). These findings suggest axonal injury related to cigarette smoking that affects neurobiological injury in AUD and hampers neurobiological recovery during abstinence (Durazzo et al., 2004; Wang et al., 2009).

Here, we used TBSS to extend our original DTI study at 1.5 T (T) (Yeh et al., 2009) by analyzing 4T DTI data obtained from smoking and non-smoking treatment seeking alcohol-dependent individuals at 1 week and 1 month of abstinence and from controls. We tested for effects of alcohol consumption, smoking and duration of abstinence from alcohol on WM microstructural measures. Based on the cited previous work, we defined a priori regions of interest (ROIs) (cingulum, corpus callosum, fornix, hippocampus, internal and external capsules, and superior longitudinal fasciculus) and expected regional WM microstructural abnormalities to be related to drinking and smoking severities. We specifically hypothesized that:

1 1-week-abstinent, treatment-seeking alcohol dependent individuals (ALC) have microstructural WM abnormalities compared with controls that correlate with measures of lifetime substance use history.
2 1-week-abstinent ALC have greater microstructural WM abnormalities than 1-month-abstinent ALC.
3 Among ALC at 1-month of abstinence and CON, cigarette smokers show greater microstructural WM abnormalities than non-smokers.

2. Methods

2.1. Participants

Structural MRI and DTI datasets were analyzed from ALC at approximately 1 week (1wkALC, n = 20) and 1 month (1moALC, n = 52) of abstinence, including both current cigarette smokers (sALC) and non-smokers (nsALC). Of these, 12 ALC had data sets at both time points, whereas 40 ALC had their first assessment at approximately 1 month of abstinence. Thirty control participants (CON, both smokers and non-smokers) were chosen from a larger group of community recruits and were matched to the ALC participants on age, gender, and smoking status. Participants were excluded for all neurological or psychiatric disorders known to affect neurobiology or cognition, except cigarette smoking. In addition, ALC were excluded for a history of illicit drug dependence in the past 5 years. Further inclusion and exclusion criteria were described (Durazzo et al., 2004). The male ALC participants were required to consume >150 alcoholic drinks per month for at least 8 years before treatment, whereas female ALC participants consumed >80 drinks per month for at least 6 years before treatment. A lifetime history of alcohol consumption was obtained (Skinner and Sheu, 1982; Sobell and Sobell, 1990; Sobell et al., 1988), self-reported impulsivity was measured using the Barratt Impulsivity Scale (BIS-11) (Patton et al., 1995), and participants completed standardized questionnaires assessing depressive [Beck Depression Inventory, BDI; (Beck, 1978)] and anxiety symptomatologies [State-Trait Anxiety Inventory, STAI; (Spielberger et al., 1977)], as well as nicotine dependence [Fagerstrom Tolerance Test for Nicotine Dependence, FTND; (Heatherton et al., 1991)]. Basic

Table 1
Demographics and clinical measures of study populations: alcohol-dependent individuals at 1 week (1wkALC) and 1 month of abstinence (1moALC) and healthy controls (CON) (mean ± standard deviation). BDI: Beck Depression Inventory; BIS: Barratt Impulsiveness Scale; FTND: Fagerstrom Test for Nicotine Dependence; STAI: Spielberger State Trait Anxiety Index. $p < 0.05$ for all the listed group comparisons. NS: not significant.

	1wkALC		1moALC		CON		
	Non-smokers	Smokers	Non-smokers	Smokers	Non-smokers	Smokers	Group comparisons
Number of participants (females)	8 (2)	12 (2)	22 (5)	30 (2)	12 (2)	18 (1)	
Duration of Abstinence [days]	11.8 ± 2.7	9.2 ± 7.1	30.9 ± 9.4	34.4 ± 6.9			
Age [years]	52.5 ± 13.7	51.7 ± 6.3	52.3 ± 13.5	48.4 ± 9.2	51.3 ± 10.1	50.3 ± 10.8	NS
1-year average drinks/month[a]	298 ± 106	373 ± 170	295 ± 156	332 ± 214	18 ± 16	23 ± 22	CON < 1moALC ($p = 0.003$)
Lifetime average drinks/month[a]	182 ± 102	250 ± 132	155 ± 86	178 ± 115	21 ± 14	26 ± 14	1wkALC > 1moALC ($p = 0.029$) CON < 1wkALC, 1moALC ($p < 0.001$)
FTND Total		4.7 ± 1.8		4.4 ± 1.5		4.5 ± 1.3	NS
Cigarettes/day		17.2 ± 7.2		15.6 ± 7.9		21.5 ± 9.3	NS
Years of smoking at current level		16 ± 12.2		18.6 ± 13.4		12.6 ± 14.9	NS
Total lifetime years of smoking		25.2 ± 10.1		28.6 ± 11		27.1 ± 13.1	NS
Recency of smoking [min]		37.8 ± 37.1		63.3 ± 39.4		29.7 ± 15.4	CON < 1moALC ($p = 0.003$)
BDI	11 ± 6.3	16.5 ± 9.1	9.8 ± 8.8	13.3 ± 8.7	4.3 ± 3.4	5.4 ± 5.1	CON < 1wkALC, 1moALC ($p < 0.001$)
BIS-11 Total	61.6 ± 8.4	61.8 ± 1.9	63.3 ± 7.8	65.2 ± 12.5	54.9 ± 11.1	60.8 ± 10.9	CON < 1moALC, NS for others
BIS-11 – Attention	15.8 ± 3.1	16.6 ± 3.5	17.1 ± 4.7	17.2 ± 4.5	13.7 ± 4.1	14.4 ± 4.2	CON < 1moALC, NS for others
BIS-11 – Motor	22 ± 3	20.2 ± 5.2	22.1 ± 3.7	23.1 ± 5.4	20.6 ± 4.1	22.8 ± 3.5	NS
BIS-11 – Non-planning	23.8 ± 3.6	25 ± 2.6	24.5 ± 4	24.9 ± 5.1	20.4 ± 3.8	23.7 ± 5.7	NS
STAI – State	38.8 ± 14	42.1 ± 15.8	34.9 ± 11.6	35.5 ± 11.3	24.6 ± 6.7	28.5 ± 6.1	CON < 1wkALC, 1moALC ($p < 0.003$)
STAI – Trait	46.1 ± 5.2	51.7 ± 14.2	45.9 ± 9.2	45 ± 12.5	31.8 ± 7.2	33.3 ± 8.2	CON < 1wkALC, 1moALC ($p < 0.001$)

[a] 1 alcoholic drink contains 13.6 g of ethanol.

demographics, substance use and behavioral measures as a function of group and smoking status are summarized in Table 1.

2.2. MR data acquisition

A 4T Bruker MedSpec system with a Siemens Trio console was used for acquiring MR images (Siemens, Erlangen, Germany) with an 8-channel transmit-receive head coil. The T1 data ($1 \times 1 \times 1\,mm^3$) were acquired with a 3D sagittal magnetization prepared rapid gradient echo, and the T2 data ($0.9 \times 0.9 \times 3\,mm^3$) were acquired with a 2D axial turbo-spin echo sequence. A dual spin echo echo planar imaging sequence was used to acquire the diffusion-weighted data (TE = 77 ms, TR = 6000 ms, flip angle of 90°), using six diffusion-encoding directions at b = 800 s/mm^2 and one at b = 0 s/mm^2. The DTI data were acquired with a nominal in-plane resolution of $2 \times 2\,mm^2$ from 40 3-mm-thick interleaved slices (no gap). To reduce geometrical distortions, twofold parallel imaging acceleration was applied. Four scans were averaged after acquisition to boost signal-to-noise. Further details have been reported (Kuceyeski et al., 2013).

2.3. DTI data processing

2.3.1. Pre-processing. The T1 and T2 images of each case were preprocessed through an expectation maximization segmentation (EMS) algorithm (Van Leemput et al., 1999a,b), which entailed bias correction and skull stripping for T1 and resampling and reslicing for T2 images. The diffusion-weighted data were pre-processed through an in-house python-based pipeline (TEEM) (http://teem.sourceforge.net/), where the DTI data was up-scaled onto the processed T1 image, and the processed T2 image was registered to the b = 0 image for geometric distortion correction. A b = 0 mask was automatically generated by TEEM, and any distortions or inaccuracies were manually corrected. After masking, the b = 0 image was then registered to the processed T1 image. The eigenvectors, diffusion tensor, and FA for each voxel were computed, and quality controls were conducted to confirm accuracy for each final FA map. Only the cases satisfying all quality control criteria were included in the TBSS analyses. An approximately equal proportion of cases (7–10%) failed quality control criteria across the three groups, which were either FA values in non-brain regions or poor registration between the T2 mask and the T1 image or between the T2 mask and the b = 0 image.

2.3.2. Tract-based spatial statistics (TBSS). All FA maps were processed via FSL's TBSS (Smith et al., 2006) for voxel-wise group-level analysis. First, individual images were aligned through a nonlinear transformation algorithm to the FMRIB58_FA template (http://fsl.fmrib.ox.ac.uk/fsl/fslwiki/FMRIB58_FA); the template contains 58 high-resolution FA volumes from healthy male and female subjects aged 20–50 years. Next, all warped FA images were normalized to the Montreal Neurological Institute standard space (MNI152 T1, 1 mm spatial resolution). A mean FA image was created from all data in the datasets and thinned to generate a mean FA skeleton that represents the locally maximal FA values. The mean FA skeleton was thresholded at FA > 0.20 to reduce partial volume effects between the borders of different tissues, yielding a subject-specific skeleton of approximately 80,000 voxels. The partial volume effects were further reduced by projecting the regional maximal FA values onto the skeleton according to a distance map (Smith et al., 2006). The resulting mean FA skeletons were fed into voxel-wise permutation-based cross-subject statistics. To compare FA values and test our hypotheses across the entire brain, voxel-wise statistics were conducted with 5000 permutations on two data sets: (1) 20 1wkALC, 52 1moALC, and 30 CON; (2) 22 nsALC and 30 sALC at 1 month of abstinence, using the FSL Randomise program (Randomise v2.9, http://fsl.fmrib.ox.ac.uk/fsl/fslwiki/Randomise) (Nichols and Holmes, 2002), and with

threshold-free cluster enhancement (TFCE) to control type I error (Smith and Nichols, 2009).

2.4. Statistical analyses

For the significant clusters in the voxel-wise statistics ($p < 0.05$ uncorrected), the FA values were extracted via the FSL cluster program (http://fsl.fmrib.ox.ac.uk/fsl/fslwiki/Cluster), with the corresponding fiber tracts identified on the Johns Hopkins WM label atlas (JHU-ICBM-DTI-81, http://cmrm.med.jhmi.edu/) (Mori et al., 2005). To assess cross-sectional differences between 20 1wkALC and 30 CON, a drinking status (ALC or CON) × smoking status (smoker or non-smoker) analysis of covariance (ANCOVA) investigated the interaction and the main effects, with age as covariate. To assess longitudinal change between time points, for 20 1wkALC and 52 1moALC, a smoking status (smoker or non-smoker) × time point (1 week or 1 month) ANCOVA investigated the interaction and the main effects, with age and average monthly drinks over lifetime as covariates; for the 12 ALC individuals with data at both time points, a paired Student *t*-test was also conducted. To assess cigarette smoking effects in 52 ALC at 1 month of abstinence and in 30 CON, a smoking status (smoker or non-smoker) × drinking status (ALC or CON) ANCOVA was performed with age as covariate. In all analyses, for clusters within the a priori ROIs (bilateral cinguli, hippocampi, internal and external capsules, and superior longitudinal fasciculi as well as genu, body, and splenium of the corpus callosum, and fornix) additional FWE corrections across space (threshold-free cluster enhancement, TFCE) corrected for the size of the skeleton in the ROI and then corrected for the number of the ROIs (n = 14, FDR-corrected $p = 0.027$); for significant clusters ($p < 0.05$ uncorrected) from the whole-brain analysis not hypothesized a priori, the *p*-values were corrected for multiplicity of the new regions using false discovery rate (FDR) statistics (Benjamini and Hochberg, 1995).

Pearson's partial correlations were computed with age as covariate to investigate associations between cluster-specific FA and measures of behavior (self-reported impulsivity, depressive and anxiety symptomatologies) and substance use; the corresponding *p*-values were corrected with family-wise error (FWE). R 3.2.0 was used for all statistical analyses (R Foundation for Statistical Computing, 2012).

3. Results

3.1. Comparisons of ALC at 1 week of abstinence versus CON

The voxel-wise statistics showed that regional FA was significantly lower ($p < 0.05$ uncorrected) in 20 1wkALC than 30 CON in clusters within the a priori ROIs of the corpus callosum (body, genu, and splenium), bilateral hippocampi, right external and internal capsules, and right superior longitudinal fasciculus (see Fig. 1). After extracting the FA values for these clusters, a 2 × 2 ANCOVA with age as a covariate showed no significant drinking status x smoking status interaction. Additional corrections for the size of these clusters across ROI space (TFCE) and for the number of a priori ROIs (FDR) yielded significant clusters (corrected) for a main effect of drinking status in the body of the corpus callosum ($F(1.48) = 15.38$, $p < 0.001$), right cingulum ($F(1.48) = 6.65$, $p = 0.013$), right external capsule ($F(1.48) = 9.73$, $p = 0.003$), and the right hippocampus ($F(1.48) = 10.96$, $p = 0.002$). The whole-brain analyses revealed additional clusters ($p < 0.05$ uncorrected) not hypothesized a priori (in anterior and posterior corona radiata, cerebellar peduncle, and thalamic radiation), but none of these remained significant after TFCE and FDR corrections. There was no significant main smoking effect and no confounding effect of recency of smoking on regional FA in any of these ROIs. Table 2 depicts detailed pairwise group comparisons.

Similar to the regions of FA differences, the uncorrected voxel-wise statistics showed higher MD in 1wkALC compared to CON, in the body of the corpus callosum, right cingulum, right external capsule, and the right hippocampus. However, none of these regional differences survived TFCE and FDR corrections for multiple comparisons.

3.2. Comparisons of ALC at 1 week versus 1 month of abstinence

The 2 × 2 ANCOVA with age and average monthly drinks over lifetime as covariates showed no significant interactions between time and smoking status on regional FA measures. None of the main effects of time or smoking status survived rigorous TFCE and FDR correction, nor did the differences in recency of smoking and average alcoholic drinks per month over lifetime confound the results (see Table 3). In additional planned pairwise comparisons of regions in which FA was significantly decreased at 1 week of abstinence, 12 ALC with measurements at both time points showed significant differences of FA at 1 week versus 1 month of abstinence within the right cingulum (0.73 ± 0.09 versus 0.79 ± 0.08) and right hippocampus (0.39 ± 0.09 versus 0.46 ± 0.08, both paired $p = 0.039$). No other brain regions showed changes with time that survived our statistical corrections.

Similar to the regions of FA differences, the uncorrected voxel-wise statistics showed higher MD in 1wkALC compared to 1moALC, in the right cingulum and right hippocampus. However, none of these regional differences survived TFCE and FDR corrections for multiple comparisons.

3.3. Comparisons of ALC at 1 month of abstinence versus CON

A 2 × 2 ANCOVA with age as covariate showed no significant interactions between drinking status and smoking status on regional FA of 1moALC and CON. There were main effects of drinking status for the body of the corpus callosum, the right cingulum and external capsule, but only the main effect within the body of the corpus callosum remained significant after rigorous TFCE and FDR corrections as described above ($F(1.80) = 10.63$, $p = 0.002$); follow-up pairwise t statistics demonstrated significantly lower FA in nsALC versus sCON (0.63 ± 0.07 versus 0.69 ± 0.07, $p = 0.02$) and sALC versus sCON (0.62 ± 0.09 versus 0.69 ± 0.07, $p = 0.004$). There was no significant main effect of smoking status and no confounding effect of recency of smoking on these measures.

2 × 2 ANCOVA with age as a covariate showed no significant drinking status × smoking status interaction for any of the regional MD measures. After TFCE and FDR correction, a significant MD difference remained between 1moALC and CON in a large cluster ($\sim 3862\ mm^3$) spanning the corpus callosum (body: $F(2.79) = 7.07$, $p = 0.005$, with age as significant covariate; genu: $F(1.80) = 9.92$, $p = 0.002$) and the anterior corona radiata (left: $F(1.80) = 16.60$, $p < 0.001$; right: $F(1.80) = 11.55$, $p = 0.001$) (see Table 4). No smoking status effect, however, survived corrections for multiple comparisons. Recency of smoking (different between 1moALC and CON, see Table 1) did not confound the results.

3.4. Associations between regional DTI metrics and behavioral outcome measures

Pearson's partial correlations with age as covariate showed in CON lower depressive symptomatology (BDI) ($r = -0.58$, $p = 0.001$) and lower total impulsivity (BIS) ($r = -0.56$, $p = 0.004$) related to higher FA within the right hippocampus. In a subset of 18 sCON, total lifetime years of smoking ($r = -0.664$, $p = 0.004$) associated negatively with FA in the genu of the corpus callosum (see Fig. 2A).

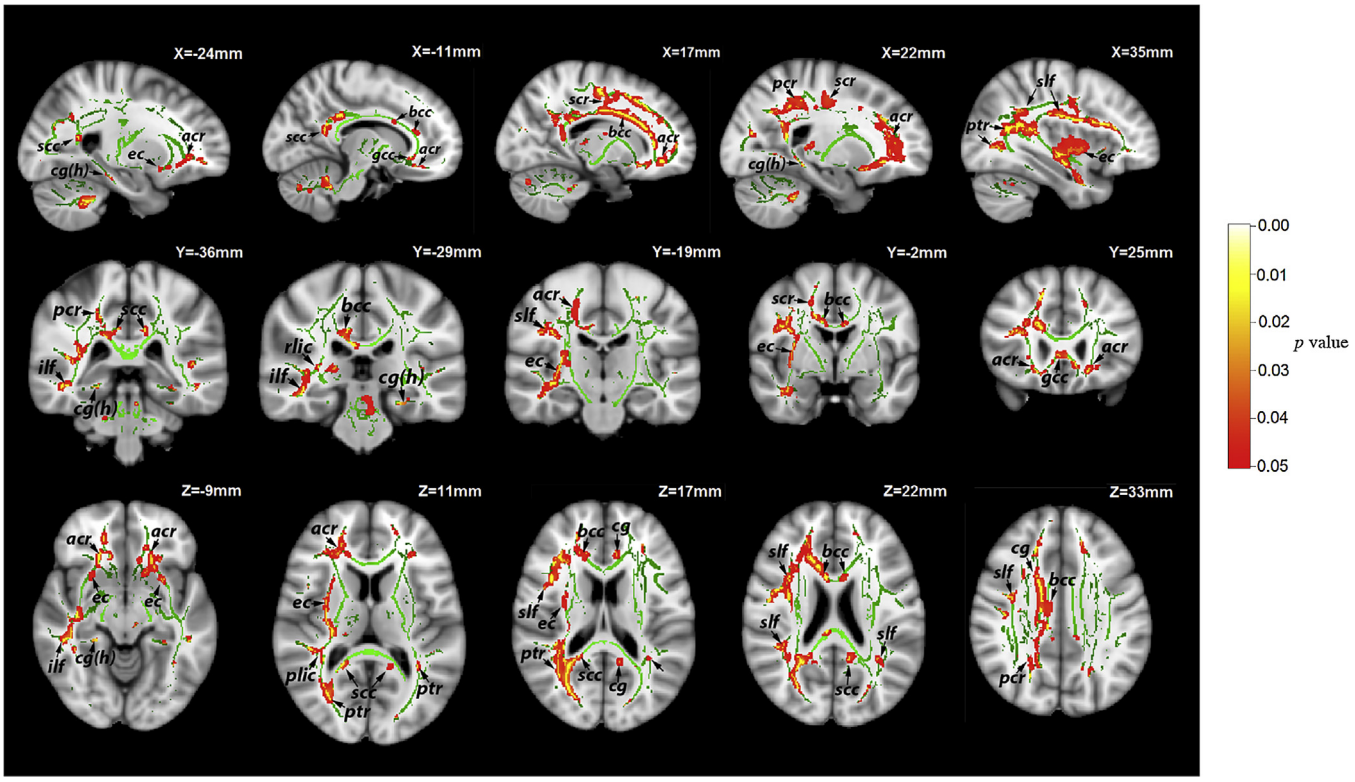

Fig. 1. Tract-Based Spatial Statistics showing FA differences in ALC at 1 week of abstinence compared to CON. All clusters are uncorrected *t*-statistical maps (Red-yellow, $p < 0.05$) of FA group differences (1wkALC < CON). The mean FA skeleton (green) is overlaid on the MNI template ($1 \times 1 \times 1\ mm^3$) and displayed in sagittal, coronal, and axial views. The number at the top-right corner indicates the distance (in mm) from the anterior commissure. *acr* = anterior corona radiata, *bcc* = body of corpus callosum, *cg* = cingulum in gyrus, *cg(h)* = cingulum in hippocampus, *ec* = external capsule, *gcc* = genu of corpus callosum, *ilf* = inferior longitudinal fasciculus. *scc* = splenium of corpus callosum, *pcr* = posterior corona radiata, *ptr* = posterior thalamic radiation, *rlic* = retrolenticular internal capsule, *scr* = superior corona radiata, *slf* = superior longitudinal fasciculus.

Table 2
Regional FA (raw mean ± standard deviation) in ALC at 1 week of abstinence and CON. Pairwise *t*-statistics are for clusters within a priori ROIs (with FDR correction, bolded when significant at $p < 0.027$); R: right hemisphere.

Tract Name	F	*p*	1wkALC		CON		*p*-value					
			nsALC (n = 8)	sALC (n = 12)	nsCON (n = 12)	sCON (n = 18)	nsALC vs. nsCON	nsALC vs. sALC	nsALC vs. sCON	sALC vs. nsCON	nsCON vs. sCON	sALC vs. sCON
Corpus Callosum – body	F(1,48) = 15.38	<0.001	0.63 ± 0.08	0.57 ± 0.08	0.67 ± 0.08	0.69 ± 0.07	0.221	0.121	0.064	**0.003**	0.525	**<0.001**
Cingulum R	F(1,48) = 6.65	0.013	0.75 ± 0.06	0.69 ± 0.11	0.80 ± 0.05	0.79 ± 0.14	0.311	0.202	0.435	**0.013**	0.722	**0.017**
External Capsule R	F(1,48) = 9.73	0.003	0.32 ± 0.03	0.33 ± 0.04	0.36 ± 0.03	0.36 ± 0.06	0.063	0.784	**0.020**	0.076	0.684	**0.020**
Hippocampus R	F(1,48) = 10.96	0.002	0.40 ± 0.11	0.36 ± 0.07	0.45 ± 0.07	0.46 ± 0.09	0.204	0.403	0.066	**0.021**	0.572	**0.003**

Table 3
Regional FA (raw mean ± standard deviation) in ALC at 1 week and 1 month of abstinence. The overall F and *p*-values are for the main effect of time. pairwise *t*-statistics for clusters within a priori ROIs (with FDR correction, bolded when significant at $p < 0.027$).

Tract Name	F	*p*	nsALC		sALC		*p*-value					
			1wk (n = 8)	1mo (n = 22)	1wk (n = 12)	1 m (n = 30)	1wkNS vs. 1mNS	1mNS vs. s1mS	1wkS vs. 1mNS	1wkNS vs. 1mS	1wkNS vs. 1wkS	1wkS vs. 1mS
Corpus Callosum – body	F(1,70) = 1.91	0.171	0.63 ± 0.08	0.63 ± 0.07	0.57 ± 0.08	0.62 ± 0.09	0.938	0.629	0.049	0.794	0.137	0.093
Cingulum R*	F(2,69) = 3.44	0.171	0.87 ± 0.18	0.86 ± 0.27	0.80 ± 0.21	0.87 ± 0.29	0.869	0.600	0.115	0.842	0.165	0.039
External Capsule R*	F(2,69) = 5.73	0.193	0.39 ± 0.08	0.41 ± 0.12	0.40 ± 0.10	0.41 ± 0.13	0.382	0.563	0.501	0.190	0.792	0.239
Hippocampus R	F(1,70) = 4.51	0.037	0.40 ± 0.11	0.44 ± 0.09	0.36 ± 0.07	0.42 ± 0.09	0.262	0.423	**0.023**	0.547	0.426	0.080

* Adjusted mean ± standard deviation with age as significant covariate at $p < 0.05$; R: right hemisphere.

Similarly, in 1wkALC, higher BDI and higher STAI trait anxiety scores correlated with lower FA in the splenium of the corpus callosum and right posterior thalamic radiation, but these correlations did not survive FWE corrections. As hypothesized, average monthly drinks over lifetime in 1wkALC correlated negatively with FA in the left external capsule, right anterior corona radiata (see Fig. 2B), and right inferior longitudinal fasciculus (all $r < -0.500$, $p < 0.03$). Similar correlations of BDI, STAI, and lifetime drinking measures existed among 1moALC, but they did not survive rigorous FWE corrections. Similar to our findings in sCON, total lifetime years smoking in 30

Table 4
Regional MD ($\times 10^{-3}$, mean ± standard deviation) in ALC at 1 month of abstinence and CON. The overall F and *p*-value is for the main effect of drinking; the MD measures are listed for each group. Pairwise *t*-statistics are for clusters within a priori ROIs with FDR correction (bolded when significant at $p < 0.027$) or from whole-brain analysis with FDR correction (bolded when significant at $p < 0.038$).

Tract Name	F	*p*	1mALC		CON		*p*-value					
			nsALC (n = 22)	sALC (n = 30)	nsCON (n = 12)	sCON (n = 18)	nsALC vs. nsCON	nsALC vs. sALC	nsALC vs. sCON	sALC vs. nsCON	nsCON vs. sCON	sALC vs. sCON
Anterior Corona Radiata R	F(1,80) = 11.55	0.001	1.3 ± 0.5	1.3 ± 0.4	0.9 ± 0.2	1.1 ± 0.4	**0.010**	0.968	0.040	**0.007**	0.443	0.032
Anterior Corona Radiata L	F(1,80) = 16.60	<0.001	1.6 ± 0.7	1.4 ± 0.4	1.1 ± 0.3	1.0 ± 0.2	**0.002**	0.049	**0.000**	0.085	0.610	**0.010**
Corpus Callosum – body*	F(2,79) = 7.07	0.005	0.7 ± 1.0	0.6 ± 1.1	0.4 ± 0.8	0.4 ± 0.9	0.051	0.657	0.038	0.091	0.914	0.072
Corpus Callosum – genu	F(1,80) = 9.92	0.002	1.5 ± 0.7	1.5 ± 0.6	1.1 ± 0.2	1.1 ± 0.4	0.032	0.704	**0.018**	0.052	0.976	0.029

* Indicates adjusted mean ± standard deviation with age as significant covariate at $p < 0.05$, group-wise *p*-values. R/L: right/left hemisphere.

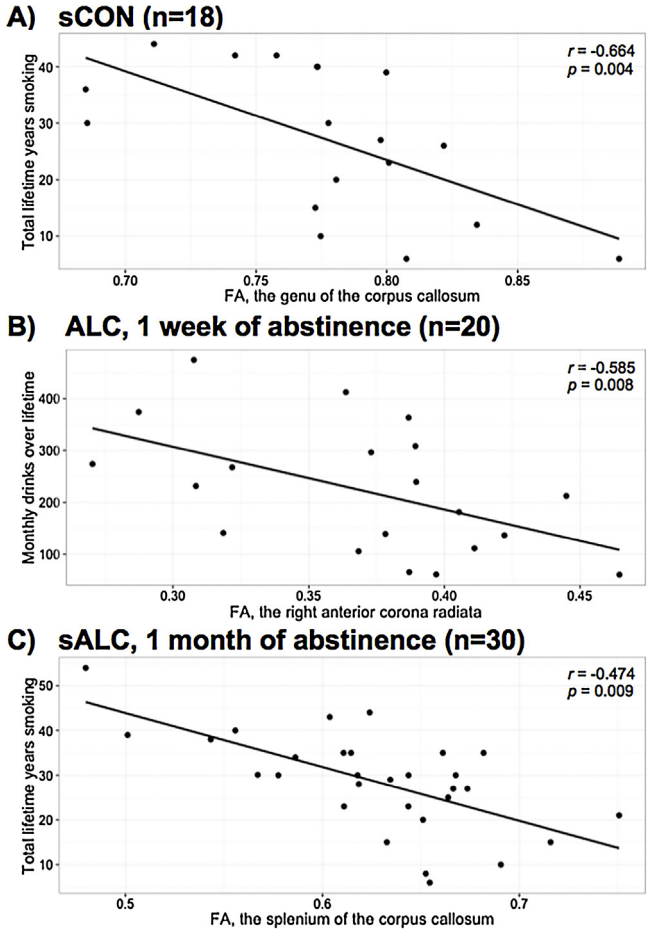

Fig. 2. Associations between smoking or drinking severities (*y*-axis) and regional fractional anisotropy (FA, *x*-axis). (A) total lifetime years of smoking related to regional FA in the genu of the corpus callosum, in 18 smoking controls (sCON); (B) monthly drinks over lifetime related to regional FA in the right anterior corona radiata, in 20 ALC at 1 week of abstinence; (C) total lifetime years of smoking related to regional FA in the splenium of the corpus callosum, in 30 smoking ALC (sALC) at 1 month of abstinence. Pearson's partial correlation coefficients (*r*) and the corresponding *p*-values are given.

sALC at one month of abstinence correlated with lower FA in the splenium of the corpus callosum ($r = -0.474$, $p = 0.009$, see Fig. 2C), whereas more cigarettes smoked per day related to higher FA in the left anterior internal capsule ($r = 0.451$, $p = 0.014$).

Within 1wkALC and 1moALC, none of the correlations between regional MD and measures of smoking severity, self-reported impulsivity, and STAI survived FWE corrections. In CON, higher MD in the corpus callosum related to lower BIS total impulsivity ($r = -0.58$, $p = 0.002$), driven by a significant correlation with non-planning impulsivity ($r = -0.51$, $p = 0.009$); these correlations, although counter-intuitive, survived FWE corrections.

4. Discussion

This study indicates widespread microstructural abnormalities of the WM in alcohol dependence but also WM microstructural recovery during short-term abstinence from alcohol. Specifically, our analyses revealed low FA values in corpus callosum and right cingulum, external capsule, and hippocampus of 1-week-abstinent ALC. All regional FA deficits except that in the body of the corpus callosum normalized after 1 month of abstinence from alcohol.

Across the alcohol dependent sample at the two time points, widespread FA reductions and MD increases were readily observable in many small clusters of different regions. However, when comparing 1moALC to CON, corrections across space for the size of the skeleton in the affected ROIs plus the corrections for the number of the ROIs analyzed retained significant FA deficits only in the body of the corpus callosum while significantly higher MD survived only in the body and genu of the corpus callosum and the anterior corona radiata. The study was also designed to measure the separate effects of chronic cigarette smoking on WM microstructure; however, none of the smoking main effects survived corrections across space and multiple measurements, suggesting that smoking affects fiber bundles heterogeneously across space within different individuals, making group differences difficult to detect in voxel wise group analyses. In addition, there were many group-specific correlations of regional FA and MD measures with substance use, mood, and impulsivity measures, highlighting the clinical significance of these DTI metrics. However, only few correlations survived FWE corrections: average monthly alcohol consumption over lifetime correlated with lower regional FA in 1wkALC, and smoking duration related to lower FA in the corpus callosum of 1moALC and CON.

A previous 1.5 T DTI study from our group compared 11 1wkALC to 10 CON and found significant FA deficits in ALC within corticostriatal fibers, limbic pathways, and frontal WM fiber bundles (Yeh et al., 2009). In that study, the ALC were mostly smokers, whereas CON were mostly non-smokers, so that smoking may have confounded the group differences. Here we obtained DTI data at higher magnetic field (4T) with better signal-to-noise, from smaller voxels and larger sample sizes and from both smoking and non-smoking ALC and CON. Serial DTI data from ALC also allowed assessing effects of abstinence on WM microstructure as a function of smoking status. Our new data suggest that chronic smoking did not contribute significantly to the microstructural group differences presented earlier (Yeh et al., 2009).

Consistent with our 1.5T TBSS study (Yeh et al., 2009), we found significantly lower FA in 1wkALC than CON (Fig. 1) within similar tracts previously reported (Pfefferbaum et al., 2006; Harris et al., 2008; Durkee et al., 2013; Pfefferbaum et al., 2014; Segobin et al., 2015; Sorg et al., 2015). The FA deficits imply disruptions

in these fibers due to axonal deletion (de la Monte and Kril, 2014), demyelination (Pfefferbaum and Sullivan, 2005), and/or microtubule disruptions (Mayfield et al., 2002), which can impair inhibitory control (Baler and Volkow, 2006), working memory, and visuospatial performance in alcohol-dependent individuals (Pfefferbaum et al., 2006).

Within most of the clusters described above, FA was higher in ALC at 1 month versus 1 week of abstinence, significant for right cingulum and hippocampus in paired comparisons, indicating microstructural recovery into the range of CON. Similar recovery of WM microstructure in ALC has been reported using other analysis methods (Gazdzinski et al., 2010; Pfefferbaum et al., 2014). Longitudinal recovery was also reported for WM volumes in ALC over 7.5 months of abstinence (Durazzo et al., 2015) and for the WM microstructure in ALC who abstained for ten years (Pfefferbaum et al., 2014). Taken together, these macro- and microstructural findings suggest remyelination of WM tracts (Sullivan and Pfefferbaum, 2005) and/or glial cell proliferation in WM during alcohol abstinence (Crews and Nixon, 2009).

Contrary to the strong effects of alcohol dependence (Table 2), smoking had nonsignificant group effects on WM microstructure and on its regional changes with abstinence in ALC. However, smoking duration correlated significantly with lower FA in the corpus callosum of both 1moALC and sCON. Just one cluster showed higher FA in smokers within the left superior corona radiata, similar to a recent TBSS study of young smokers (Yu et al., 2015). Our finding of lower FA within the splenium of the corpus callosum of sALC versus nsALC is consistent with a previous smoking study in controls (Savjani et al., 2014). However, these clusters of smoking related group differences did not survive our rigorous statistical tests in this analysis.

In CON, we found negative associations of depressive symptomatology, self-reported impulsivity, and smoking duration with regional FA, suggesting that microstructural measures have behavioral correlates in CON. Similar correlations in ALC did not survive FWE corrections, except for negative relationships of lifetime alcohol consumption and smoking duration to regional FA. These rather weak correlations in ALC may be related to greater individual variability of FA measures and their changes during recovery. Furthermore, previous cross-sectional DTI studies revealed no significant associations between cigarette smoking measures and regional FA among non-alcoholic individuals (Fritz et al., 2014) or male heavy drinkers (Monnig et al., 2015). Those studies recruited different populations, e.g., in Monnig's study, not all the heavy drinkers were diagnosed with AUD, more than half were young adults with relatively short smoking durations, and the average number of cigarettes per smoking day was relatively low. However, significantly lower concentrations of NAA were detected within the frontal WM of 1-week-abstinent smoking ALC compared to non-smoking ALC and non-smoking CON (Durazzo et al., 2013) as well as in the anterior corona radiata of 1-month-abstinent smoking ALC compared to non-smoking controls (Wang et al., 2009). Taken together, although group differences related to smoking were not significant during early abstinence from alcohol or in controls, significant relationships within smoking groups suggest some detrimental effects of chronic smoking on WM microstructure.

This study bears several limitations. The number of ALC participants per group was limited by the availability of 4T DTI data at the different time points and by our stringent QC criteria. Males dominated the participants in both ALC and CON and we could not study sufficient numbers of ALC at 1 week of abstinence, which complicated our longitudinal analyses. Diffusion was encoded in only 6 directions as we initiated the studies more than ten years ago; this does allow TBSS analyses but not more detailed tractography as enabled by more modern DTI sequences that encode at least 30 directions (Mukherjee et al., 2008). Further, TBSS has several technical challenges (Bach et al., 2014): the orientation information is discarded when computing the skeletal FA map, therefore anatomical connectivity between different brain regions cannot be analyzed; TBSS cannot resolve merging or crossing fibers where diffusion metrics derived from the tensors do not properly represent the WM microstructure (Wheeler-Kingshott and Cercignani, 2009; Jbabdi et al., 2010; Jeurissen et al., 2013). In addition, we did not separately explore the less commonly examined subcomponents of FA and MD, axial and radial diffusivity, given cautionary statements in the literature (e.g., Wheeler-Kingshott and Cercignani, 2009).

Altogether, our investigations clarify some behavioral correlates of WM microstructural abnormalities in abstinent alcohol dependent individuals. At treatment entry, their microstructure was compromised within frontal WM, cortico-striatal and limbic fiber bundles, significantly correlated with alcohol drinking and weakly related to mood symptoms and self-reported impulsivity. Over approximately 1 month of abstinence, abnormal WM microstructural metrics in several regions recovered into the range of healthy controls. Overall, cigarette smoking did not influence strongly our cross-sectional group comparisons or changes of DTI metrics during abstinence. However, since in both smoking CON and smoking 1moALC lower FA in corpus callosum related to smoking measures, smoking cessation may improve FA deficits in smokers. The weak associations of lower FA with poorer behavioral measurements (i.e., self-reported impulsivity) in ALC at both 1 week and 1 month of abstinence suggest that ALC may benefit from cognitive-based therapy aimed at maintaining abstinence. Finally, if the WM microstructural measures reflect myelin status, ALC may benefit from pharmacology that supports remyelination.

Conflict of interest

No conflict declared.

Contributors

Drs. Dieter Meyerhoff and Timothy Durazzo had central oversight and overall responsibility for this research that included study participants from different but related research projects. Drs. Timothy Durazzo, Donna Murray and Dieter Meyerhoff were responsible for MR data acquisition. Mr. Thomas Schmidt was responsible for obtaining demographic, behavioral and cognitive data, supervised by Dr. Durazzo. Dr. Murray and Mr. Troy Murray participated in data pre-processing. Mr. Yukai Zou was responsible for data preparation, processing and statistical analyses under the supervision of Drs. Murray and Meyerhoff. Mr. Zou did the literature review and wrote the first draft of the manuscript. All authors approved the final version of the manuscript.

Role of funding source

This investigation was supported by the NIH AA10788 (DJM) and DA024136 (TCD).

Acknowledgements

We extend our appreciation to all participants who volunteered for this study. We thank Derek Flenniken for his assistance with diffusion data processing. For patient recruitment we thank Mary Rebecca Young, Bill Clift, Kathleen Altieri, Ricky Chen, and Drs. Peter Banys, Steven Batki, and Ellen Herbst of the Veterans Administration Substance Abuse Day Hospital, and Dr. David Pating, Karen Moise, and colleagues from the Kaiser Permanente Chemical Dependency Recovery Program in San Francisco.

References

Bühler, M., Mann, K., 2011. Alcohol and the human brain: a systematic review of different neuroimaging methods. Alcohol Clin. Exp. Res. 35, 1771–1793.

Bach, M., Laun, F.B., Leemans, A., Tax, C.M., Biessels, G.J., Stieltjes, B., Maier-Hein, K.H., 2014. Methodological considerations on tract-based spatial statistics (TBSS). Neuroimage 100, 358–369.

Baler, R.D., Volkow, N.D., 2006. Drug addiction: the neurobiology of disrupted self-control. Trends Mol. Med. 12, 559–566.

Basser, P., Mattiello, J., Le Bihan, D., 1994. MR diffusion tensor spectroscopy and imaging. Biophys. J. 66, 259–267.

Beaulieu, C., 2002. The basis of anisotropic water diffusion in the nervous system—a technical review. NMR Biomed. 15, 435–455.

Benjamini, Y., Hochberg, Y., 1995. Controlling the false discovery rate: a practical and powerful approach to multiple testing. J. R. Stat. Soc. 57, 289–300.

Bolego, C., Poli, A., Paoletti, R., 2002. Smoking and gender. Cardiovasc. Res. 53, 568–576.

Crews, F.T., Nixon, K., 2009. Mechanisms of neurodegeneration and regeneration in alcoholism. Alcohol Alcohol. 44, 115–127.

de la Monte, S.M., Kril, J.J., 2014. Human alcohol-related neuropathology. Acta Neuropathol. 127, 71–90.

Danaei, G., Ding, E.L., Mozaffarian, D., Taylor, B., Rehm, J., Murray, C.J., Ezzati, M., 2009. The preventable causes of death in the United States: comparative risk assessment of dietary, lifestyle, and metabolic risk factors. PLoS Med. 6, e1000058.

Demirakca, T., Ende, G., Kammerer, N., Welzel-Marquez, H., Hermann, D., Heinz, A., Mann, K., 2011. Effects of alcoholism and continued abstinence on brain volumes in both genders. Alcohol Clin. Exp. Res. 35, 1678–1685.

Durazzo, T.C., Meyerhoff, D.J., 2007. Neurobiological and neurocognitive effects of chronic cigarette smoking and alcoholism. Front. Biosci. 12, 4079–4100.

Durazzo, T.C., Gazdzinski, S., Banys, P., Meyerhoff, D.J., 2004. Cigarette smoking exacerbates chronic alcohol- induced brain damage: a preliminary metabolite imaging study. Alcohol Clin. Exp. Res. 28, 1849–1860.

Durazzo, T.C., Mon, A., Gazdzinski, S., Meyerhoff, D.J., 2013. Chronic cigarette smoking in alcohol dependence: associations with cortical thickness and N-acetylaspartate levels in the extended brain reward system. Addict. Biol. 18, 379–391.

Durazzo, T.C., Mattsson, N., Weiner, M.W., 2014a. Alzheimer's Disease Neuroimaging Initiative,. Smoking and increased Alzheimer's disease risk: a review of potential mechanisms. Alzheimers Dement. 10, S122–S145.

Durazzo, T.C., Mon, A., Pennington, D., Abé, C., Gazdzinski, S., Meyerhoff, D.J., 2014b. Interactive effects of chronic cigarette smoking and age on brain volumes in controls and alcohol-dependent individuals in early abstinence. Addict. Biol. 19, 132–143.

Durazzo, T.C., Mon, A., Gazdzinski, S., Yeh, P.H., Meyerhoff, D.J., 2015. Serial longitudinal magnetic resonance imaging data indicate non-linear regional gray matter volume recovery in abstinent alcohol-dependent individuals. Addict. Biol. 20, 956–967.

Durkee, C.A., Sarlls, J.E., Hommer, D.W., Momenan, R., 2013. White matter microstructure alterations, a study of alcoholics with and without post-traumatic stress disorder. PLoS One 8, e80952.

Fortier, C.B., Leritz, E.C., Salat, D.H., Lindemer, E., Maksimovskiy, A.L., Shepel, J., Williams, V., Venne, J.R., Milberg, W.P., McGlinchey, R.E., 2014. Widespread effects of alcohol on white matter microstructure. Alcohol Clin. Exp. Res. 38, 2925–2933.

Fritz, H.C., Wittfeld, K., Schmidt, C.O., Domin, M., Grabe, H.J., Hegenscheid, K., Hosten, N., Lotze, M., 2014. Current smoking and reduced gray matter volume-a voxel-based morphometry study. Neuropsychopharmacology 39, 2594–2600.

Garey, K.W., Neuhauser, M.M., Robbins, R.A., Danziger, L.H., Rubinstein, I., 2004. Markers of inflammation in exhaled breath condensate of young healthy smokers. Chest 125, 22–26.

Gazdzinski, S., Durazzo, T.C., Mon, A., Yeh, P.H., Meyerhoff, D.J., 2010. Cerebral white matter recovery in abstinent alcoholics – a multimodality magnetic resonance study. Brain 133, 1043–1053.

Giovino, G.A., 2002. Epidemiology of tobacco use in the United States. Oncogene 21, 7326–7340.

Harris, G.J., Jaffin, S.K., Hodge, S.M., Kennedy, D., Caviness, V.S., Marinkovic, K., Papadimitriou, G.M., Makris, N., Oscar-Berman, M., 2008. Frontal white matter and cingulum diffusion tensor imaging deficits in alcoholism. Alcohol Clin. Exp. Res. 32, 1001–1013.

Hawkins, B.T., Brown, R.C., Davis, T.P., 2002. Smoking and ischemic stroke: a role for nicotine. Trends Pharmacol. Sci. 23, 78–82.

Heatherton, T.F., Kozlowski, L.T., Fracker, R.C., Fagerström, K.O., 1991. The Fagerström Test for Nicotine Dependence: a revision of the Fagerström Questionnaire. Br. J. Addict. 86, 1119–1127.

Hudkins, M., O'Neill, J., Tobias, M.C., Bartzokis, G., London, E.D., 2012. Cigarette smoking and white matter microstructure. Psychopharmacology (Berl.) 221, 285–295.

Jbabdi, S., Behrens, T.E.J., Smith, S.M., 2010. Crossing fibres in tract-based spatial statistics. NeuroImage 49, 249–256.

Jeurissen, B., Leemans, A., Tournier, J., Jones, D.K., Sijbers, J., 2013. Investigating the prevalence of complex fiber configurations in white matter tissue with diffusion magnetic resonance imaging. Hum. Brain Mapp. 34, 2747–2766.

Kuceyeski, A., Meyerhoff, D.J., Durazzo, T.C., Raj, A., 2013. Loss in connectivity among regions of the brain reward system in alcohol dependence. Hum. Brain Mapp. 34, 3129–3142.

Liao, Y., Tang, J., Deng, Q., Deng, Y., Luo, T., Wang, X., Chen, H., Liu, T., Chen, X., Brody, A.L., Hao, W., 2011. Bilateral fronto-parietal integrity in young chronic cigarette smokers, a diffusion tensor imaging study. PLoS One 6, e26460.

Lin, F., Wu, G., Zhu, L., Lei, H., 2013. Heavy smokers show abnormal microstructural integrity in the anterior corpus callosum: a diffusion tensor imaging study with tract-based spatial statistics. Drug Alcohol Depend. 129, 82–87.

Mayfield, R.D., Lewohl, J.M., Dodd, P.R., Herlihy, A., Liu, J., Harris, R.A., 2002. Patterns of gene expression are altered in the frontal and motor cortices of human alcoholics. J. Neurochem. 81, 802–813.

Meyerhoff, D.J., 2014. Brain proton magnetic resonance spectroscopy of alcohol use disorders. Handb. Clin. Neurol. 125, 313–337.

Miller, B.L., 1991. A review of chemical issues in 1H NMR spectroscopy: *N*-Acetyl-*L*-aspartate, creatine and choline. NMR Biomed. 4, 47–52.

Monnig, M.A., Yeo, R.A., Tonigan, J.S., McCrady, B.S., Thoma, R.J., Sabbineni, A., Hutchison, K.E., 2015. Associations of white matter microstructure with clinical and demographic characteristics in heavy drinkers. PLoS One 10, e0142042.

Mori, S., Wakana, S., Nagae-Poetscher, L.M., van Zijl, P.C.M., 2005. MRI Atlas of Human White Matter. Elsevier, Amsterdam: Elsevier.

Mori, S., Zhang, J., 2006. Principles of diffusion tensor imaging and its applications to basic neuroscience research. Neuron 51, 527–539.

Mukherjee, P., Berman, J.I., Chung, S.W., Hess, C.P., Henry, R.G., 2008. Diffusion tensor MR imaging and fiber tractography: theoretic underpinnings. AJNR. Am. J. Neuroradiol. 29, 632–641.

National Institute on Alcohol Abuse and Alcoholism (NIAAA), 2015. Alcohol Facts and Statistics, Retrieved 6 April 2016. From http://www.niaaa.nih.gov/alcohol-health/overview-alcohol-consumption/alcohol-facts-and-statistics.

Nichols, T.E., Holmes, A.P., 2002. Nonparametric permutation tests for functional neuroimaging: a primer with examples. Hum. Brain Mapp. 15, 1–25.

Oscar-Berman, M., Marinkovic, K., 2003. Alcoholism and the brain: an overview. Alcohol Res. Health 27, 125–133.

Patton, J.H., Stanford, M.S., Barratt, E.S., 1995. Factor structure of the Barratt impulsiveness scale. J. Clin. Psychopharmacol. 51, 768–774.

Paul, R.H., Grieve, S.M., Niaura, R., David, S.P., Laidlaw, D.H., Cohen, R., Sweet, L., Taylor, G., Clark, R.C., Pogun, S., Gordon, E., 2008. Chronic cigarette smoking and the microstructural integrity of white matter in healthy adults: a diffusion tensor imaging study. Nicotine Tob. Res. 10, 137–147.

Pfefferbaum, A., Sullivan, E.V., 2005. Disruption of brain white matter microstructure by excessive intracellular and extracellular fluid in alcoholism: evidence from diffusion tensor imaging. Neuropsychopharmacology 30, 423–432.

Pfefferbaum, A., Lim, K.O., Zipursky, R.B., Mathalon, D.H., Rosenbloom, M.J., Lane, B., Ha, C.N., Sullivan, E.V., 1992. Brain gray and white matter volume loss accelerates with aging in chronic alcoholics: a quantitative MRI study. Alcohol Clin. Exp. Res. 16, 1078–1089.

Pfefferbaum, A., Adalsteinsson, E., Sullivan, E.V., 2006. Dysmorphology and microstructural degradation of the corpus callosum: interaction of age and alcoholism. Neurobiol. Aging 27, 994–1009.

Pfefferbaum, A., Rosenbloom, M.J., Chu, W., Sassoon, S.A., Rohlfing, T., Pohl, K.M., Zahr, N.M., Sullivan, E.V., 2014. White matter microstructural recovery with abstinence and decline with relapse in alcohol dependence interacts with normal ageing: a controlled longitudinal DTI study. Lancet Psychiatry 1, 202–212.

R Foundation for Statistical Computing, 2012. R: A Language and Environment for Statistical Computing, Vienna, Austria https://www.r-project.org/.

Rohlfing, T., Sullivan, E.V., Pfefferbaum, A., 2006. Deformation-based brain morphometry to track the course of alcoholism: differences between intra-subject and inter-subject analysis. Psychiatry Res. 146, 157–170.

Romberger, D.J., Grant, K., 2004. Alcohol consumption and smoking status: the role of smoking cessation. Biomed. Pharmacother. 58, 77–83.

Savjani, R.R., Velasquez, K.M., Thompson-Lake, D.G., Baldwin, P.R., Eagleman, D.M., De La Garza 2nd, R., Salas, R., 2014. Characterizing white matter changes in cigarette smokers via diffusion tensor imaging. Drug Alcohol Depend. 145, 134–142.

Schuff, N., Ezekiel, F., Gamst, A.C., Amend, D.L., Capizzano, A.A., Maudsley, A.A., Weiner, M.W., 2001. Region and tissue differences of metabolites in normally aged brain using multislice 1H magnetic resonance spectroscopic imaging. Magn. Reson. Med. 45, 899–907.

Segobin, S., Ritz, L., Lannuzel, C., Boudehent, C., Vabret, F., Eustache, F., Beaunieux, H., Pitel, A.L., 2015. Integrity of white matter microstructure in alcoholics with and without Korsakoff's syndrome. Hum. Brain Mapp. 36, 2795–2808.

Skinner, H.A., Sheu, W.J., 1982. Reliability of alcohol use indices. The lifetime drinking history and the MAST. J. Stud. Alcohol. 43, 1157–1170.

Smith, S.M., Nichols, T.E., 2009. Threshold-free cluster enhancement: addressing problems of smoothing, threshold dependence and localization in cluster inference. Neuroimage 44, 83–98.

Smith, S.M., Jenkinson, M., Johansen-Berg, H., Rueckert, D., Nichols, T.E., Mackay, C.E., Watkins, K.E., Ciccarelli, O., Cader, M.Z., Matthews, P.M., Behrens, T.E., 2006. Tract-based spatial statistics: voxelwise analysis of multi-subject diffusion data. Neuroimage 31, 1487–1505.

Smith, K.W., Gierski, F., Andre, J., Dowell, N.G., Cercignani, M., Naassila, M., Duka, T., 2015. Compromised microstructural integrity in corpus callosum in binge males, which is linked with impaired cognitive functioning. Addict. Biol., http://dx.doi.org/10.1111/adb.12332, Epub ahead of print.

Sobell, L.C., Sobell, M.B., 1990. Self-report issues in alcohol abuse: state of the art and future directions. Behav. Assess. 12, 91–106.
Sobell, L.C., Sobell, M.B., Riley, D.M., Schuller, R., Pavan, D.S., Cancilla, A., Klajner, F., Leo, G.I., 1988. The reliability of alcohol abusers' self-reports of drinking and life events that occurred in the distant past. J. Stud. Alcohol 49, 225–232.
Sorg, S.F., Squeglia, L.M., Taylor, M.J., Alhassoon, O.M., Delano-Wood, L.M., Grant, I., 2015. Effects of aging on frontal white matter microstructure in alcohol use disorder and associations with processing speed. J. Stud. Alcohol Drugs 76, 296–306.
Sullivan, E.V., Pfefferbaum, A., 2005. Neurocircuitry in alcoholism: a substrate of disruption and repair. Psychopharmacology (Berl.) 180, 583–594.
Sullivan, E.V., 2000. NIAAA Research Monograph No. 34: human brain vulnerability to alcoholism: evidence from neuroimaging studies. In: Noronha, A., Eckardt, M., Warren, K. (Eds.), Review of NIAAA's Neurosciences and Behavioral Research Portfolio. National Institute on Alcohol aAbuse and Alcoholism, Bethesda, MD, pp. 473–508.
Trivedi, R., Bagga, D., Bhattacharya, D., Kaur, P., Kumar, P., Khushu, S., Tripathi, R.P., Singh, N., 2013. White matter damage is associated with memory decline in chronic alcoholics: a quantitative diffusion tensor tractography study. Behav. Brain Res. 250, 192–198.
Van Leemput, K., Maes, F., Vandermeulen, D., Suetens, P., 1999a. Automated model-based bias field correction of MR images of the brain. IEEE Trans. Med. Imaging 18, 885–896.
Van Leemput, K., Maes, F., Vandermeulen, D., Suetens, P., 1999b. Automated model-based tissue classification of MR images of the brain. Med. Imaging IEEE Trans. Med. Imaging 18, 897–908.
Wang, J.J., Durazzo, T.C., Gazdzinski, S., Yeh, P.H., Mon, A., Meyerhoff, D.J., 2009. MRSI and DTI: a multimodal approach for improved detection of white matter abnormalities in alcohol and nicotine dependence. NMR Biomed. 22, 516–522.
Wheeler-Kingshott, C.A.M., Cercignani, M., 2009. About axial and radial diffusivities. Magn. Reson. Med. 61, 1255–1260.
Wozniak, J.R., Lim, K.O., 2006. Advances in white matter imaging: a review of in vivo magnetic resonance methodologies and their applicability to the study of development and aging. Neurosci. Biobehav. Rev. 30, 762–774.
Xiao, P., Dai, Z., Zhong, J., Zhu, Y., Shi, H., Pan, P., 2015. Regional gray matter deficits in alcohol dependence: a meta-analysis of voxel-based morphometry studies. Drug Alcohol Depend. 153, 22–28.
Yeh, P.H., Simpson, K., Durazzo, T.C., Gazdzinski, S., Meyerhoff, D.J., 2009. Tract-Based Spatial Statistics (TBSS) of diffusion tensor imaging data in alcohol dependence: abnormalities of the motivational neurocircuitry. Psychiatry Res. 173, 22–30.
Yu, D., Yuan, K., Zhang, B., Liu, J., Dong, M., Jin, C., Luo, L., Zhai, J., Zhao, L., Zhao, Y., Gu, Y., Xue, T., Liu, X., Lu, X., Qin, W., Tian, J., 2015. White matter integrity in young smokers: a tract-based spatial statistics study. Addict. Biol. 21, 679–687, http://dx.doi.org/10.1111/adb.12237.
Zahr, N.M., 2014. Structural and microstructural imaging of the brain in alcohol use disorder. Handb. Clin. Neurol. 125, 275–290.
Zhang, X., Salmeron, B.J., Ross, T.J., Geng, X., Yang, Y., Stein, E.A., 2011. Factors underlying prefrontal and insula structural alterations in smokers. Neuroimage 54, 42–44.